A fully distributed hierarchical control framework for coordinated operation of DERs in active distribution power networks

Shiwei Xia, *Member, IEEE*, S. Q. Bu, *Senior Member, IEEE*, Can Wan, *Member, IEEE*, Xi Lu, Ka Wing Chan, *Member, IEEE*, and Bin Zhou, *Senior Member, IEEE*

Abstract—In order to effectively accommodate large-scale DERs in active distribution power networks, this paper proposes a fully distributed hierarchical framework to economically manage multiple DERs within three layers: the tertiary, the secondary generation regulation layer and the primary frequency droop control layer. In the tertiary layer, a fully distributed dispatch strategy is designed to optimally allocate the active power base point of DERs in a center-free manner, with total generation and load imbalance locally estimated by individual DER using the discrete finite-time consensus algorithm. In the secondary layer, a distributed fair generation correction strategy is designed based on power sharing ratio to timely counterbalance the load deviations on top of the tertiary layer. In the primary layer, a droop controller is presented for DER, battery energy storage and controllable load to maintain satisfactory system frequency performance. The proposed hierarchical framework is a fully distributed generation coordinating approach, which could optimally control active power outputs of multiple DERs with the minimal cost while ensuring satisfactory system frequency, and is also robust to DERs' uncertainties. Case studies have demonstrated the effectiveness of proposed fully distributed hierarchical framework for optimally coordinating DERs power outputs and regulating system frequency.

Index Terms—active distribution power network, distributed energy resources, hierarchical control framework, generation correction strategy

I. INTRODUCTION

With the development of renewable energy generation technology, distributed energy resources (DERs) such as wind power generation, photovoltaic power generation and gas-fired generation etc., are extensively integrated into distribution networks. This requires a change in the paradigm of distribution power network from conventional passive into active, thus resulting in the active distribution power network (ADPN), in order to reduce the negative impacts of DERs and effectively manage DERs in a large scale [1]. In addition, current smart grid technologies such as the information and communication technology (ICT) and the multi-agent technology make it possible to proactively coordinate DERs operating in an optimal manner [2]. It is necessary to develop a general paradigm with suitable control strategies for the coordinated operation of DERs to achieve better power quality and more economical operation for the whole network.

Conventional optimization methods for distribution network operation are mainly centralized, which rely on a powerful hub to collect global information of all components and conduct the computational procedure. However, because of the ever-growing penetration level and the distributed nature of DERs, centralized strategies are going to encounter some technical challenges [3]. Firstly, the large volume of data caused by DERs' integration will result in the heavy computational burden and communication complexity of control center. Then, the system is susceptible to single-point-failure. Moreover, the plug-and-play operational requirements of DERs are unable to be flexibly satisfied. Therefore, the fully distributed strategies are preferred for their superiorities of scalability, sparse network, and improved resiliency to faults or unknown parameters [4, 5].

Recently, some studies have applied distributed algorithms in solving economic dispatch (ED) problems [4, 5]. For instance, in [7] a decentralized ED approach was proposed based on generators' incremental costs and a leader agent was used to collect the global generation and load demand information for calculating the power mismatch. In [8] the average consensus strategy was used for the local estimation of power mismatch shared among distributed generators, and a novel distributed dispatch algorithm was established for solving the ED problem. In [9, 10], a fully distributed ED algorithm was proposed by using an additional innovation term to ensure that the power mismatch gradually approaches to zero. In [11], the consensus algorithm was hybrid with the alternating direction method of multipliers (ADMM) for solving the optimal power flow problem with demand response in a distributed manner. The above literatures mainly focused on applying distributed algorithms for off-line optimal operation of DERs in tertiary generation regulation layer, while the off-line solutions are not suitable to be implemented for the real-time coordination of DERs in distribution networks.

As a complement to the off-line optimization in a single layer, some scholars have put forward the hierarchical control structure to address different requirements with different control hierarchy. For example, authors of [12] proposed a hierarchical control scheme to improve the system overall efficiency while considering the State-of-Charge balance at the same time, while the secondary and tertiary control were implemented in a micro-grid central controller. In [13], a potential-function was used for the secondary and tertiary control of a micro-grid, and an all-round central controller was needed to communicate with all DERs. Besides of these centralized hierarchical control schemes for power system operation, some center-free hierarchical control strategies were also put forward. For instance, a decentralized hierarchical framework was proposed in [14] and [15] to optimize the charging process of PEVs for frequency regulation in a competitive electricity market. In [16, 17], new distributed control strategies were established for both the frequency and voltage regulation of micro grids, in which only the localized information and nearest-neighbor communication were needed. Dr. M. A. Mahmud of [18] designed a nonlinear distributed controller capable of maintaining both active and reactive power balance to prevent overloading. Further, the work in [19] is not only able to restore the system frequency and network voltage in a distributed manner but also ensure its reactive power sharing. However, the above works mainly perform the power quality regulation and solve the power sharing problem proportionally according to DERs' power ratings, while the economical operation of the whole system is not taken into account and thus optimal power sharing cannot be achieved.

Motivated by the above works, this paper proposed a fully distributed hierarchical control framework for optimally coordinating DERs operation in ADPN by three layers. In the tertiary generation regulation layer, a fully distributed dispatch

strategy incorporating the ADMM into discrete finite-time consensus algorithm (DFCA) was properly designed to optimize the active power base point of DERs in a center-free manner. In the secondary generation regulation layer, a distributed fair generation correction strategy was proposed by using the DFCA to counterbalance the load deviations in a shorter timescale on top of the tertiary generation regulation, which was also without relying on a central coordinator. Collectively, the tertiary and secondary layers provided the primary control layer with active power tracking reference points. In the primary layer, by using locally measured frequency deviations, the power droop controller was designed for the fast acting devices including the DERs, battery energy storages (ESs) and the controllable load to maintain satisfactory frequency dynamic performance of ADPN. In this way, all the three layers are designed to operate without a central coordinator and therefore a fully distributed hierarchical control framework is well established.

The main contributions of this paper are as follows.

1) To accommodate the feature of highly penetrating and widely scattering DERs, a fully distributed hierarchical framework without requiring a centralized coordinator, as comparisons to the centralized hierarchical framework in [12, 13] or decentralized one in [14, 15], is innovatively designed for ADPN economical operation by using ADMM and DFCA for the tertiary and secondary layer as well as the local droop controller for the primary layer, respectively.

Compared with ordinary consensus based ADMM for DC-OPF problem [11], here the DFCA is incorporated into ADMM for formulating an efficient distributed optimization algorithm with less complexity and good data privacy, which only needs very few iterations to calculate the power imbalances in tertiary layer compared with the ordinary consensus algorithm as demonstrated by Fig.5. Different from the conventional centralized generation correction approach implemented with a control center to collect fuel cost coefficients of all DERs for calculating power participation factors [20], the DFCA is utilized in this paper to form a distributed generation correction strategy and conduct the economical generation correction without any central controller in the secondary layer.

2) The proposed fully distributed framework could optimally control the active power output of multiple DERs with the minimal cost under the fluctuating load condition, while ensuring satisfactory system dynamic frequency performance. Compared with the distributed control scheme in [4, 16-19] to conduct the generation corrections according to its rated power, which neglected the economy of the generation corrections in the secondary layer, the proposed distributed approach utilizes the DFCA to realize the economical generation corrections in the secondary layer and thereby the corporation of tertiary and secondary layer can obtain the real time optimal solution of DERs outputs, which has been validated by the benchmark results of traditional centralized methods. (please refer to the Table 1 in page 7).

3) The proposed hierarchical framework is robust to accommodate the complexities and uncertainties of DERs, such as the random plug-in/out behaviors of DERs.

4) Comprehensive simulations on a distribution system with multiple DERs have demonstrated that the proposed fully distributed hierarchical framework is effective to optimally coordinate the power output of DERs and can well regulate the system frequency.

The rest of this paper is organized as follows. The preliminary of DERs' economically coordinated operation and the discrete finite-time algorithm are introduced in Section II,

and then a fully distributed three-layer hierarchical control framework is designed in Section III. Afterwards three case studies are conducted in Section IV and V to validate the effectiveness of the proposed hierarchical scheme, and the conclusion is drawn in the last section.

II. PRELIMINARY

This section first presents the problem formulation of DERs coordinated operation, and then the background of discrete time finite algorithm used for dispatching DERs in the later section is introduced. It is also noted that the ramping constraints, startup/shutdown constraints etc. of DERs could be readily handled by many techniques in a multiple timescale paradigm including the day-ahead security constrained unit commitment and the real time security constrained unit commitment (several hours ahead) [21, 22], these constraints are not considered in this paper due to the page limits and the focus of this research is to optimally coordinate DERs operation for a short timescale, in specific from 5 minutes approaching the real time.

A. problem formulation of DERs' coordinated operation

The emerging generation technologies have enriched the diversities of DERs, which could be generally categorized into dispatchable and non-dispatchable. The gas-fired power generator and diesel combustion turbines etc. with good controllability are the common dispatchable DERs, while the photovoltaic generators and wind power generators etc. highly relying on intermittent renewable energy sources driven by weather are the common non-dispatchable DERs. In this paper, non-dispatchable DERs will be treated as negative loads, and their actual power outputs are formed in terms of power generation predictions plus generation deviations. The purpose of DERs coordinated operation is to effectively and economically control the dispatchable DERs in ADPN to match conventional load demands and the negative load demands for non-dispatchable DERs in real time.

Assume n dispatchable DERs in ADPN, the objective of DERs coordinated operation is to minimize the total generation cost, i.e.,

$$\min \sum_{i=1}^{n} F_i(G_i) = \min \sum_{i=1}^{n} (a_i G_i^2 + b_i G_i + c_i) \qquad (1)$$

where $F_i(G_i)$ is the fuel cost of gas-fired power generators or diesel combustion turbines with coefficients a_i, b_i and c_i. The power balance constraint and DER output limits are for the real time load and generation balance as (2).

$$\sum_{i=1}^{n} G_i = \sum_{j}^{m} D_j \qquad (2)$$

$$P_{i\min} \leq G_i \leq P_{i\max} \qquad (3)$$

where G_i and D_j stand for the ith DER output and jth load respectively; n and m are the numbers of DERs and loads. Distinguished from the conventional ED model which only considers the offline load predictions in (2), we would like to emphasize D_j in (2) is the actual load demand in this paper and the objective of DERs coordinated operation is to optimally control a large number of DERs for the actual load demand. The real time actual load demand would be denoted by the off-line load prediction D_{prej} plus the on-line load deviation D_{devj} as (4).

$$D_j = D_{prej} + D_{devj} \qquad (4)$$

As DERs have the advantage of being flexibly ramped up/down or turned on/off, the presented model (1)-(4) could explore the fast response capability of DERs to match the real time load demands. In Section III, a fully distributed

hierarchical control scheme will be designed by economically dispatching DERs operation base point for load predictions D_{prej} in the tertiary layer plus conducting DERs generation corrections for on-line load deviations D_{devj} in the secondary generation regulation layer.

B. Discrete finite-time consensus algorithm (DFCA)

In Section III, a fully distributed control scheme will be proposed to solve the model (1)-(4) in a center-free manner. As preliminaries for designing this control scheme, the basic concept of the graph theory and discrete finite-time consensus algorithm are briefly reviewed in the following.

A graph G is usually used to represent the communication network topology coupled with power devices. The graph G is a pair of set (V_G, E_G), where $V_G =\{ V_1 ,V_2 ,...,V_n \}$ is the non-empty set for vertices and $E_G =\{e_1,e_2,...,e_k\}$ is the set for edges with $e_k=(V_i ,V_j)$. N_i is the set of neighbor agents of agent i. The adjacency matrix A of G is a $n{\times}n$ symmetric matrix with elements $a_{ij}=a_{ji}=1$ if $j{\in}N_i$, otherwise $a_{ij} =a_{ji}=0$. The Laplacian matrix L of G is formed with $l_{ii}=\sum a_{ij}$ ($j{\in}N_i$) and $l_{ij}=-a_{ij}$ ($j{\neq}i$).

The conventional consensus algorithm is described as [7]

$$y_i^{(k)} = \omega_{ii} y_i^{(k-1)} + \sum_{j \in N_i} \omega_{ij}(y_i^{(k-1)} - y_j^{(k-1)}) \quad (5)$$

where $y_i^{(k)}$ is the physical state of agent i at iteration k, ω_{ii} and ω_{ij} are the weighting factors of agent i and neighbor agent j, respectively.

Lemma [23, 24]: If $\lambda_2 \neq \lambda_3 \neq ... \neq \lambda_{K+1} \neq 0$ be the K distinct nonzero eigenvalues of the Laplacian matrix L, then y_i in (5) would converge to the average value in K steps, i.e., $y_i^{(k)} = y_j^{(k)} = (\sum_{i=1}^n y_i^{(0)})/n$, if the weighting factors are updated as follows.

$$\omega_{ij}^{(s)} = \begin{cases} 1 - a_i/\lambda_s & (i = j) \\ 1/\lambda_s & (j \in N_i) \end{cases} \quad (s=2,...,K+1) \quad (6)$$

where $a_i =|N_i|$ is the number of neighboring agents of agent i. To implement (6), each agent needs to know the nonzero eigenvalues of Laplacian matrix L. To address this concern, a graph discovery strategy based on the network flooding method is used to determine L locally for each agent, and then the eigenvalues of L are calculated to update the weighting factors in (6) for distributed algorithms [24, 25].

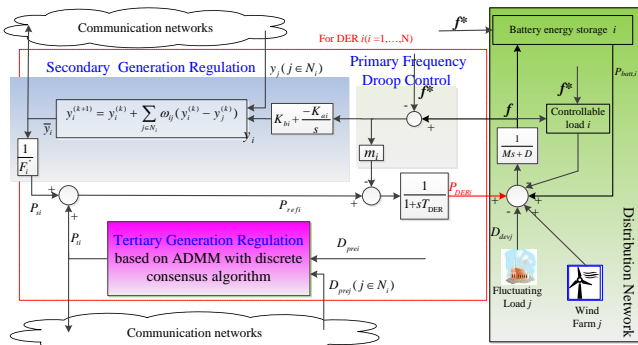### III. PROPOSED FULLY DISTRIBUTED THREE-LAYER HIERARCHICAL FRAMEWORK

Fig. 1 Proposed fully distributed hierarchical control framework

Fig. 1 depicts the proposed fully distributed hierarchical control framework for DERs coordinated operation. It has three control layers: the tertiary generation regulation layer, the secondary generation regulation layer and the droop characteristic based primary frequency control layer. The tertiary layer, which is the top and also the slowest one, is mainly concerned with the DER distributed off-line economic dispatch for predicted load demands. The secondary layer is

designed to have faster dynamics response than that of the tertiary layer and is used to conduct the generation corrections for load deviations in distributed manner. The bottom layer is the primary control which locally provides the frequency regulation and ensures reference tracking with fast responses.

In the tertiary layer, a fully distributed dispatch strategy based on DFCA is properly designed to optimally allocate the active power base point of DERs in a center-free manner. For the secondary generation regulation, a distributed fair generation correction strategy is proposed by using DFCA based on the power sharing ratio to timely counterbalance the load deviations in a shorter timescale on top of the tertiary generation regulation. Collectively, the tertiary and secondary layers provide the primary control layer with active power tracking reference points. In the primary layer, a local frequency droop controller is presented for DERs, battery energy storage and controllable load to maintain satisfactory system frequency dynamics. In the following, we will describe the three-layer generation regulation scheme in detail.

A. Distributed tertiary generation regulation

In the tertiary generation regulation layer, we designed a fully distributed optimization approach based on ADMM and DFCA to conduct the off-line generation dispatch for the predicted load D_{prej}, and this optimal generation of DER in tertiary layer is indicated as P_{ti} in Fig.1. If G_i and D_j are substituted by P_{ti} and D_{prej} in (1)-(2) for merely considering load predictions, DERs off-line generation dispatch problem could be converted to the extended Lagrangian formulation as

$$L_e = \sum_{i=1}^n (a_i P_{ti}^2 + b_i P_{ti} + c_i) + \lambda(\sum_{i=1}^n P_{ti} - \sum_{j=1}^m D_{prej}) + \frac{\rho}{2}\left\|(\sum_{i=1}^n P_{ti} - \sum_{j=1}^m D_{prej})\right\|_2^2 \quad (7)$$

where λ is the Lagrange multiplier and ρ is a positive constant parameter. As a typical decentralized algorithm, the Alternating Direction Method with Multiplier (ADMM) algorithm could solve complex optimization problems in divide-and-conquer manner and is therefore a powerful optimization engine with attractive convergence performance. According to ADMM theory [26, 27], the output of DER i is solved as

$$P_{ti}^{(k+1)} = \underset{P_{imin} \le P_{ti} \le P_{imax}}{\arg\min} \ L_e(P_{t1}^{(k)}, P_{t2}^{(k)},...,P_{t(i-1)}^{(k)}, P_{ti}, P_{t(i+1)}^{(k)},...,P_{tn}^{(k)}, \lambda^k)$$

$$= \underset{P_{imin} \le P_{ti} \le P_{imax}}{\arg\min} \ [a_i P_{ti}^2 + b_i P_{ti} + c_i + \lambda^k(\sum_{j=1}^n P_{tj}^{(k)} - P_{ti}^{(k)} + P_{ti} - \sum_j^m D_{prej})$$

$$+ \frac{\rho}{2}(\sum_{j=1}^n P_{tj}^{(k)} - P_{ti}^{(k)} + P_{ti} - \sum_j^m D_{prej}] \quad (8)$$

Denote $\sum_{j=1}^n P_{tj}^{(k)} - \sum_j^m D_{prej} = e^{(k)}$, then (8) can be simplified as

$$P_{ti}^{(k+1)} = \frac{\rho[P_{ti}^{(k)} - e^{(k)}] - \lambda^{(k)} - b_i}{\rho + 2a_i} \quad (i = 1,...,n) \quad (9)$$

with constraint $P_{imin} < P_{ti}^{(k+1)} < P_{imax}$ for i^{th} DER output P_{ti}. The dual variable is updated by

$$\lambda^{(k+1)} = \lambda^{(k)} + \rho(\sum_{i=1}^n P_{ti}^{(k+1)} - \sum_j^m D_{prej}) = \lambda^{(k)} + \rho e^{(k+1)} \quad (10)$$

Equation (9) and (10) are updated iteratively for the optimal solution until the following criterions are both satisfied [28].

$$\| r^{(k+1)} \|_2 = \rho(\sum_{i=1}^{n} P_{ti}^{(k+1)} - \sum_{j}^{m} D_{prej}) < \varepsilon^{pri}$$

$$\| s^{(k+1)} \|_2 = \sqrt{\sum_{i=1}^{n}(P_{ti}^{(k+1)} - P_{ti}^{(k)})^2} < \varepsilon^{dual} \quad (11)$$

where ε^{pri} and ε^{dual} are tolerance parameters pre-specified in terms of expected accuracy.

From formula (9), the updating of $P_{ti}^{(k+1)}$ relies on ith DER's local parameters a_i, b_i, and the system total power imbalance $e^{(k)}$. As $e^{(k)}$ is the global information of the whole system and needs to be estimated by collecting all DERs' outputs and all loads in distribution networks with an information hub, it is just a decentralized approach instead of a fully distributed one when directly using ADMM to solve the problem. A fully distributed approach should be capable of calculating the global imbalanced power $e^{(k)}$ only based on the local information without any central coordinator. For this purpose, the previous introduced DFCA in Section II.B could be introduced to estimate $e^{(k)}$ by sharing limited information with neighbor agents as below.

Algorithm 1: DFCA for locally estimating $e^{(k)}$

1) Suppose there are totally n buses connected with loads and DERs, and the power imbalance for node i is initialized as $y_i^{(0)} = P_{ti}^{(0)} - D_{prei}$, where $P_{ti}^{(0)}$ and D_{prei} stand for the DER initial output and load prediction at bus i. (Note: for a bus only with load then $P_{ti}^{(0)} = 0$, and similarly $D_{prei} = 0$ for a node only with DER). Initialize the weighting factors ω_{ij} by (5) based on the pre-configured communication network;

2) Repeat to update $y_i^{(k)}$ by DFCA using (5) in K steps, where $y_i^{(k)}$ stands for the average power imbalance estimated at bus i;

3) The total unbalanced power $e^{(k)}$ could be calculated as $n \times y_i^{(k)}$ for bus i, where n is the total number of buses.

The proposed distributed dispatch approach based on ADMM and DFCA mainly includes the following steps for the tertiary generation regulation.

1) Initialize the output of DER i as $P_{ti}^{(0)}$ and the dual variable $\lambda^{(0)}$, prepare the weighting factors ω_{ii} and ω_{ij} by (5) according to the communication network;

2) Estimate the total power imbalance $e^{(k)}$ of distributed system networks by **Algorithm 1**;

3) Update ith DER output $P_{ti}^{(k+1)}$ by (9) and the dual variable $\lambda^{(k+1)}$ by (10);

4) If the stop condition (11) is satisfied, output $P_{ti}^{(k+1)}$ as the final optimal solution; otherwise go to step 2).

B. *Distributed secondary generation regulation*

In the tertiary generation regulation, we only find the DER optimal output (called base point hereafter) for the predicted load demand D_{prej}. However, the actual load demand D_j in real time is usually different from the predicted load as expressed in (4), and our ultimate goal is to economically coordinate the DERs outputs for the real-time actual load demand.

As the tertiary layer has already optimized DER operation base point P_{ti} for the predicted load D_{prej}, if we could further conduct the economical generation correction (indicated as P_{si} here) for the real time load deviation D_{devj} on top of the base point, then the integrated generation in tertiary and secondary layer as $P_{refi} = P_{ti} + P_{si}$ would be the DER optimal solution for the real-time actual load demands. In other words, as the actual load deviates from the load prediction, we need to investigate how much each DER should be adjusted (i.e., 'participate' in the load change) from the base point in order that the actual load can be served by DERs in the most economical manner.

Assume both the first and second order derivatives of fuel cost function with respect to DER output are available (i.e., both F_i' and F_i'' exist for fuel cost function F_i in (1)). It is well-known that the incremental costs or the first order derivatives F_i' ($i=1,...n$) of all DERs are equal to the Lagrange multiplier λ when DERs reach the optimal solution. Denote the incremental cost of DER i for the base point P_{ti} in tertiary layer as $\lambda^0 = F_i'(P_{ti})$. Since the system total load is changed by a total amount of $\sum D_{devj}$, the marginal cost and optimal output of DER i should move to $\lambda^0 + \Delta\lambda$ and $P_{ti} + P_{si}$ accordingly with the relationship $\lambda^0 + \Delta\lambda = F_i'(P_{ti} + P_{si})$, then we have

$$\Delta\lambda = F_i'(P_{ti} + P_{si}) - F_i'(P_{ti}) = F_i''(P_{ti}) \times P_{si} \quad \text{for } i=1,...n \quad (12)$$

To satisfy the power generation and load balance, we have

$$\sum_{i=1}^{n} P_{si} = \sum_{j=1}^{m} D_{devj} \quad (13)$$

The solution of (12) and (13) is

$$P_{si} = pf_i \times (\sum_{j=1}^{m} D_{devj}) \quad (14)$$

where $pf_i = \dfrac{1}{F_i''} \bigg/ \sum_{j=1}^{n} \dfrac{1}{F_j''}$ is the power participation factor for DER i. Formula (14) indicates that the economical generation correction P_{si} of DER i for the total load deviation $\sum D_{devj}$ is inversely proportional to the second derivative F_i'' of fuel cost. For conventional generation correction, a central controller is needed to collect fuel cost coefficients of all DERs for calculating the summation of F_j'' ($j=1,...n$) and the power participation factors pf_i [20]. In order to design a distributed generation, formula (14) is rewritten in the form of (15) for DER i and j.

$$\sum_{j=1}^{m} D_{devj} = P_{si}/pf_i = P_{sj}/pf_j \quad \text{or} \quad y_i = P_{si}/\frac{1}{F_i''} = P_{sj}/\frac{1}{F_j''} = y_j \quad (15)$$

where y_i and y_j are the defined power sharing ratio in terms of DER generation correction to DER power participation factor. These power sharing ratios y_i and y_j are also the tailored consensus variables for DER i and j which could be used in the discrete finite-time consensus algorithm as shown in Fig.1.

With (15), the secondary regulator compares the local power sharing ratio y_i of DER i with its neighbors' power sharing ratio y_j on a communication graph and accordingly ensures all DERs' power sharing ratio converging to the consensus value in finite-time, which could be guaranteed by **Lemma** of DFCA introduced in Section II.B. Thereby the equality (15) is satisfied in finite time, and an economical generation correction strategy is established based on the power sharing ratio to timely counterbalance load deviations $\sum D_{devj}$ on top of the tertiary generation regulation layer.

To provide the input signal for secondary generation regulation in Fig.1, the frequency deviation Δf, calculated as the frequency reference f^* minus the distribution network actual frequency f, is controlled by a PI controller, which would increase or decrease the generation correction of DER i accordingly for the positive or negative frequency deviations until the frequency deviation approaches zero.

With the help of distributed tertiary and secondary generation regulation, the DER economical outputs for actual load demands mainly compose of two parts: the economic base point P_{ti} for predicted load $\sum D_{prej}$ and the economical generation corrections P_{si} for load deviation $\sum D_{devj}$. The summation $P_{ti} + P_{si}$ will provide the complete optimal power reference point P_{refi} for the primary frequency droop controller to track as shown in Fig.1.

C. Local *primary frequency regulation*

In the primary frequency regulation layer, the frequency droop controller is presented to ensure the fast acting devices can perfectly track the reference point and maintain satisfactory system frequency with quick responses. In this paper, the DERs, battery Energy Storages (ESs) and controllable load are integrated for primary frequency regulation.

1) Primary Frequency Regulation of DER

In the primary layer, we utilize the feedback of frequency deviation Δf as the input of droop controller as shown in Fig.1. Since DER with small initial belongs to the fast acting devices, a simplified first-order inertia dynamic model with small time constant is used to represent the input-output characteristics. Hence, DER dynamic model incorporating the power reference and droop control can be described by (16)

$$P_{DERi} = \frac{1}{1+sT_{DERi}} \times (P_{refi} - m_i(f*-f)) \qquad (16)$$

where T_{DERi} and m_i are the inertia time constant and droop coefficient of DER i; P_{refi} is the optimal power reference of DER i provided by the tertiary and secondary generation regulation layer; f^* and f are the frequency reference and the network actual frequency.

2) Primary Frequency Regulation of Controllable Load

With the development of smart grid paradigm, the load control on the demand side is the impressive supplement to the power generation control from the generation side. The simplest way of realizing this is by utilizing the so-called controllable load such as the combined cooling heating and power, controllable water heater etc. Due to its outstanding flexibility, the controllable load can be appropriately adjusted to reduce/increase power consuming so as to counterbalance the supply-demand imbalance [29, 30], and therefore it is very effective for frequency regulation from the load side. In this paper, the controllable load is model as one inertial block with the ramp up/down and anti-windup limits as shown in Fig.2. The input signal is the system frequency deviation and output is the controlled load (CL) demand.
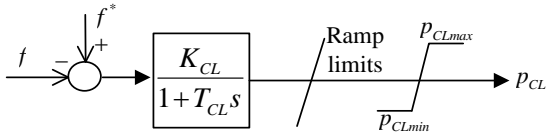

Fig. 2 Dynamic model of controllable load for frequency regulation

3) Ancillary Frequency Regulation Service of ESs

ESs are the power electronics based devices which has extremely fast response and therefore the ancillary frequency regulation service is one of the most valuable applications which could fully exploit the merits of ESs instantaneous high power. In this paper, ES is controlled with the droop characteristics against the frequency deviation, with the discharging/charging power limits and State of Charge (SOC) constraints also be satisfied during the frequency regulation procedure.

The completed ancillary frequency regulation service of ES could be described by formula (17) at the bottom of this page, where P_{ESimax}, SOC_{min} and SOC_{max} are the maximal discharging power, the minimal and maximal SOC; Δf is the frequency deviation; K_{ESi} is ES droop coefficient for frequency regulation; $P_{req,i,t}$ and SOC_t are the power reference determined by the frequency droop control which is the control signal for modeling ES dynamics in Fig.3.

The ES can be modeled as a Thevenin-based voltage source in series with an internal resistance R_{series} and a paralleled RC network (consisting of the resistance R_{trans} and capacitor C_{trans}) [31]. The terminal voltage is related to SOC and defined as a nonlinear term of SOC by Nernst equation.

$$V_{oc} = V_{nom} + \alpha(RT/F)\ln(SOC/(C_{nom}-SOC)) \qquad (18)$$

where α is a sensitivity parameter of V_{oc} to SOC; R, F and T are the gas constant, the Faraday constant and battery temperature, respectively. When SOC is kept within a range of 10%−95% to preserve battery life, R_{series}, R_{trans} and C_{trans} can be approximated as constants with typical values obtained from [31]. The dynamics of battery charging could be described by the block diagram in Fig. 3 [25], where $P_{req,i,t}$ is the reference point of ES charging/discharging power determined by the primary frequency regulation controller using (17).
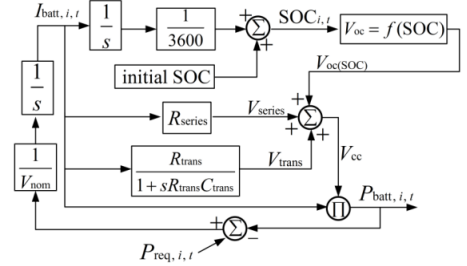

Fig. 3 Model for PEV battery charging dynamics

For the distribution network dynamic, an inertia block diagram $1/(Ms+D)$ is used to model the effect of the net load change on frequency deviation by parameter D and the inertia M of distribution network as shown in Fig.1.

Remarks:

1) Based on the proposed hierarchical framework, DER generations could be effectively coordinated based on the DFCA (in the tertiary and secondary generation regulation layer) and the local frequency droop control (in the primary frequency regulation layer), which only needs the local information and parameters without any central information hub, and hence the proposed hierarchical framework is a fully distributed control approach;

2) The proposed fully distributed hierarchical framework can optimally coordinate the active power output of multiple DERs with the minimal cost by optimizing the base point in the tertiary layer plus economically conducting generation correction in the secondary layer, while ensuring satisfactory system frequency with fast response in the primary layer.

3) The proposed distributed framework can be fitted in a two-segment power market composed of intra-day market and real-time spot market. The power generation scheduling of tertiary layer could be performed in the intra-day market based on the price signals such as the fuel costs of local generators, and the combination of ADMM and DFCA could be used to address the optimal solutions in a center-free intra-day market, in which the market participants will coordinate to make bids periodically for each timeslot (such as 5-15 minutes) without market decision center and update their generators output accordingly. The secondary and primary frequency regulation layers can be used to provide balancing services in the real-time spot market, and the generation correction and droop control strategies will be used to reallocate the supply-demand unbalance among generators and ES. While the technical content of the proposed distributed scheme is the focus here, the application of proposed scheme in a centre-free market environment will be thoroughly investigated in the future.

$$P_{req,i,t} = \begin{cases} -P_{ESi\max} & (K_{ES_i}\Delta f < -P_{ESi\max}) \,\&\, (SOC_t < SOC_{\max}) \\ K_{ES_i}(f*-f) = K_{ES_i}\Delta f & (-P_{ESi\max} < K_{ES_i}\Delta f < P_{ESi\max}) \,\&\, (SOC_{\min} < SOC_t < SOC_{\max}) \\ P_{ESi\max} & (K_{ES_i}\Delta f > P_{ESi\max}) \,\&\, (SOC_t > SOC_{\min}) \\ 0 & (K_{ES_i}\Delta f < 0) \,\&\, (SOC_t > SOC_{\max}) \\ 0 & (K_{ES_i}\Delta f > 0) \,\&\, (SOC_t < SOC_{\min}) \end{cases} \quad (17)$$

IV. CASE STUDY FOR 33-BUS ADPN WITH WIND FARMS

The performance of proposed hierarchical framework for DERs coordinated operation was firstly tested on a modified 33-bus ADPN [32] with a single Point of Common Coupling (PCC) as shown in Fig. 4, which consists of 15 DERs, 32 loads, 2 energy storages, 1 controllable load and 3 wind farms. The 15 DERs are deployed in the bus set {1, 3, 5, 7, 9, 11, 13, 15, 17, 19, 21, 23, 25, 27, 29} while the fuel cost coefficients are cited from TABLE II of [33] and the upper limits of power outputs are enlarged 2.5 times to match the system total load level. As illustrated in Fig.4, the communication links (indicated as blue dash line) are mainly configured based on the physical network, which can conveniently utilize the power line communication techniques, plus extra links between bus 8-22, 18-33, 25-29 to satisfy the n-1 communication reliability. Each bus in Fig.4 is deployed with a smart agent, which is capable of communicating with its neighbor agents for sharing the load and generation information. The tertiary generation regulation layer is updated every 300s based on the short-term load and wind power prediction, while the secondary generation regulation and the first layer control are updated in real time. The parameters of ADPN inertia block are D=1.25MW/Hz, M=50s. The droop coefficient of DERs is m_i=0.1MW/Hz. And the parameters of controllable load are K_{CL}=1.5 MW/Hz and T_{CL}=5s MW/Hz. The droop coefficient of two ESs are K_{ES1}=2 MW/Hz for K_{ES2}=1 MW/Hz.

For the parameter ρ of ADMM, as there are no general rules of how to select the optimal penalty parameter ρ, in the following case studies we choose ρ by trial and errors and fix it as 10^{-5} to guarantee the good convergence and yield the optimal solutions.
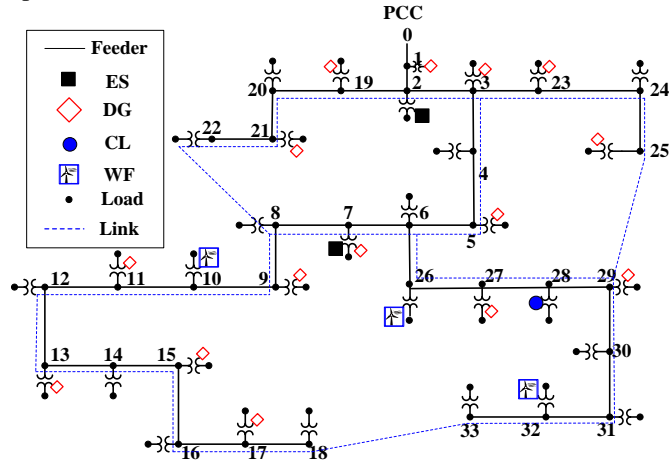

Fig.4 Modified IEEE 33-bus ADPN with 3 WFs and 15 DERs

A. Case 1: investigate the performance of proposed scheme by 33-bus ADPN with simplified load condition

For zooming in the performance of proposed scheme, we firstly conducted simulations for the following simplified scenarios: 1) To check the effectiveness of the tertiary generation regulation layer, the predicted total load level of the 33-bus ADPN is assumed as 3715kW during 0-300s, while at 300s bus1 to bus10 each increases 20kW and therefore the predicted load demand changes to 3715kW+200kW=3915kW during 300s-2400s; 2) To validate

the performance of the secondary generation correction layer, the total load deviation of this 33-bus ADPN is assumed zero during 0s-700s and 450kW during 700s-2400s, and the step moment is indicated by the blue dot-line B in Fig.5; 3) DER11 is disconnected at 1300s indicated by the blue dot-line C and reconnected at 1900s marked by the blue dot-line D in Fig.5 to investigate the robustness of proposed scheme for random plug-in/out behaviors of DERs.
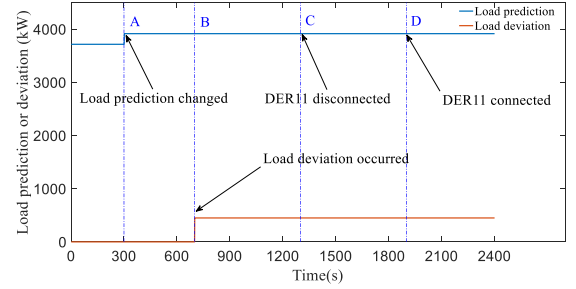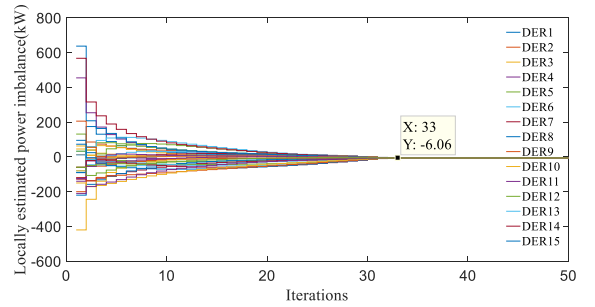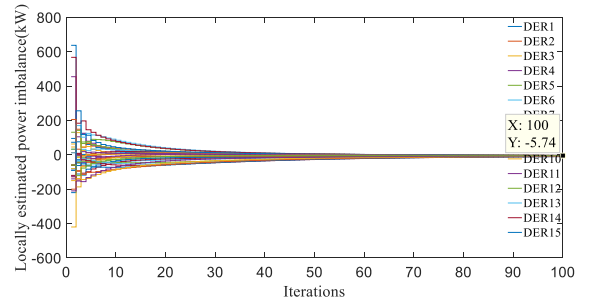

Fig.5 Simplified load conditions for 33-bus ADPN

1) Convergence of DFCA for estimating load imbalance $e^{(k)}$

a) by discrete finite-time consensus algorithm

b) by conventional consensus algorithm

Fig. 6 Convergence for estimating average load imbalance

The prowess of DFCA for locally estimating the total generation and load imbalance (described by **algorithm 1**) is firstly investigated for the stepping moment 300s, when the power imbalance 200kW occurs. Fig 6 shows the convergence performance of DFCA and the conventional consensus algorithm [7,11]. As illustrated in Fig.6a), the DFCA estimated the average load imbalance of 33 buses as 6.06kW in very fewer iterations indicating the total power imbalance (equal to the average value multiplied by total number of buses) is 6.06kW*33=199.98kW which is almost the same as the practical power imbalance 200kW. However, the conventional consensus algorithm could only reach an average estimation of 5.74kW at 100 iterations as shown in Fig. 6b) indicating a total power imbalance 5.74kW*33=189.42kW, which would converge to a satisfied estimation by several hundred iterations. This comparison shows that the DFCA is
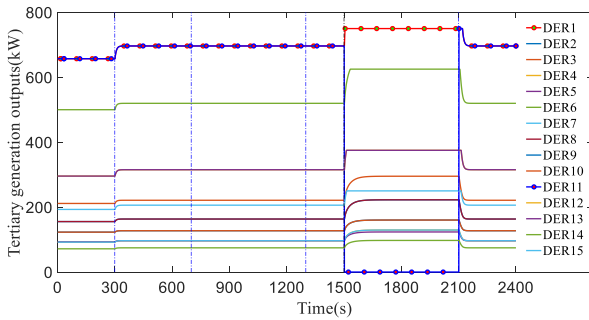
more powerful than the conventional consensus algorithm to accurately estimate the power imbalance at the cost of fewer iterations.
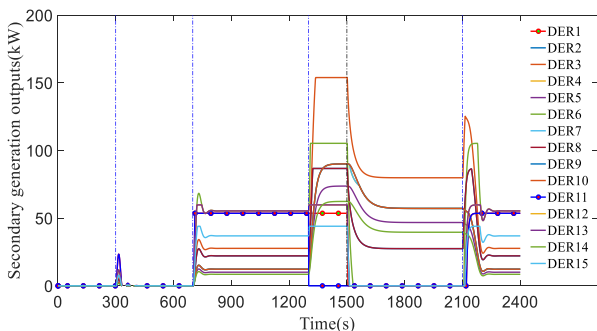
2) Optimality performance of proposed scheme

Based on the accurately estimated power imbalance, ADMM would be used to effectively seek DERs' optimal operation base point of tertiary layer. As shown in Fig.7a), when the predicted load level changes from 3715kW to 3915kW at 300s (indicated by the first blue dot-line), the ADMM approach only costs several iterations to obtain DERs optimal solutions as detailed in the second column of Table I. Due to the suddenly enlarged load demands at 300s, the system frequency is slightly reduced with the help of the primary frequency droop controller in the primary layer at first. However, the secondary generation regulation layer immediately detects the frequency droop and tries to make up the power deficiency and results in a small fleeting power perturbation nearby 300s in Fig.7b). When the load deviation 450kW occurs at 700s (at the second blue dot-lined), the secondary generation regulation layer timely conducts generation corrections to counterbalance the load deviation accordingly as shown in Fig.7b). With a short transition, all DERs generation corrections reach static until the next disturbance occurs at 1300s.
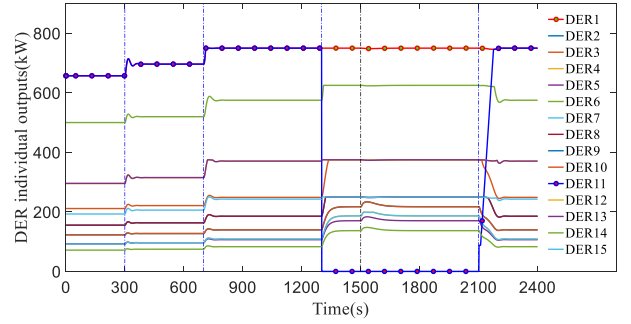
To check the global optimization capability of secondary generation regulation layer when counterbalancing load deviations, DERs optimal generation corrections in the secondary layer at 900s are detailed in the third column of Table I, while the summations of the generation corrections and the optimal base points in the tertiary layer are also shown in the forth column. Considering that we cannot accurately know the system actual load level in advance, the one-off optimized solutions of conventional centralized ED for the total load 3915kW+450kW=4365kW are used as the benchmark only for comparison purpose, which are provided in the fifth column of Table I. Compared with conventional ED solution, the proposed scheme could solve comparable DER optimal solutions with a satisfied minimal cost as shown in the last row of Table I. These comparisons indicate that the proposed scheme can effectively coordinate multiple DERs operations with the satisfactory optimality performance in a distributed manner.
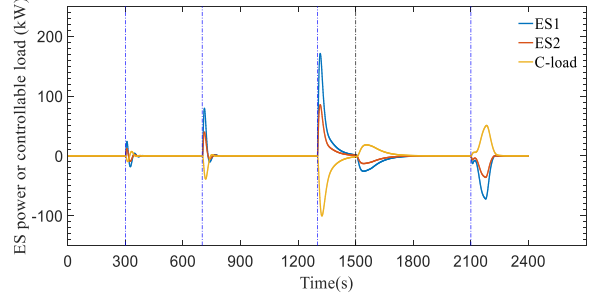

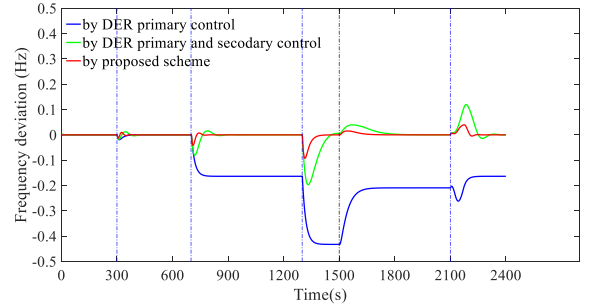a）DER optimal operation base point in tertiary layer

b) DER generation corrections in secondary layer

c) DER actual power outputs

d) Energy storage outputs and Controllable load demand

e) Frequency regulation performance

Fig.7 Performance of proposed scheme in simplified load conditions

Table I Solutions of proposed scheme and centralized ED at 900s

DER index	Proposed Scheme(kW)			Centralized ED for 4365kW (kW)
	Tertiary generation dispatch for 3915kW	Secondary generation corrections for 450kW	Individual total outputs	
1	696.62	53.38	750.00	750.00
2	163.33	22.15	185.48	185.43
3	221.12	27.72	248.83	248.78
4	96.39	12.32	108.72	108.74
5	96.46	10.09	106.55	106.60
6	519.16	55.53	574.70	575.06
7	96.31	12.35	108.66	108.74
8	163.12	22.23	185.35	185.43
9	127.23	12.35	139.58	139.57
10	127.30	12.30	139.60	139.57
11	696.62	53.38	750.00	750.00
12	315.33	55.35	370.69	370.56
13	315.32	55.35	370.67	370.56
14	74.59	8.53	83.12	83.09
15	206.11	36.96	243.07	242.88
Cost ($/h)	832.4169			832.4171

3) Robustness of proposed scheme

To investigate the robustness of proposed scheme for accommodating random plug-in/out behaviors of DERs, DER11 was disconnected at 1300s and reconnected as 1900s as indicated in Fig.5. Since the tertiary generation regulation layer updated the optimal base point every 300s while the secondary generation regulation layer conducted the generation corrections in real time, with loss of 750kW power generation at 1300s due to the disconnection of DER11, the secondary layer immediately provided the increased

generation corrections to complement the power insufficiency as shown in Fig.7b) during 1300s-1500s. Afterward at 1500s, the tertiary generation regulation layer started to take effects and re-dispatched the total predicted load 3915kW among the other 14 DERs except the DER11 as shown in Fig.7a), meanwhile the secondary layer reduced DERs generation corrections accordingly and reallocated the original load deviation 450 kW among all DERs except the DER11 at 1500s. Afterward, though DER11 was reconnected at 1900s, it was designed that the system reserves a short time interval to prepare for DER11 back, and DER11 was schedulable at the next updating interval 300s. Therefore the tertiary and secondary generation regulation layer only began to take effect at 2100s and finally reached the optimal operation points, which are exactly the same as the operation states during 700s-1300s before DER11 disconnection.

Fig. 7c) and Fig. 7d) also displayed the actual outputs of DERs, ESs and the controllable load for the aforementioned conditions during 2400s, respectively. The simulation results indicated that the DERs could always be coordinated to undertake certain amount of load demands, while for the ESs and controllable load, they only support power outputs during the transient period when the frequency deviations occur. This is because the DERs has three control layers while the ESs and controllable load only work with frequency droop controller for primary frequency regulation.

In order to demonstrate the functionality of the secondary layer, the ESs and controllable load in the primary layer, the following three schemes are implemented separately for frequency regulation. 1) the ED algorithm with DERs primary frequency droop control; 2) the proposed three-layer hierarchical control scheme excluding the primary frequency droop control of ESs and controllable load; 3) the proposed completed three-layer hierarchical control scheme. As shown in Fig.7e), the Scheme 1) has large frequency deviations when the load unbalance occurs since 700s, while for scheme 2) and 3), their frequency deviations are zero during most of time and they only slightly fluctuate with many small burrs at the ephemeral power imbalance moment. This is because both scheme 2) and 3) have the generation corrections in the secondary layer and therefore they could well compensate the power imbalance. When further make comparisons between scheme 2) and 3), it is clear that scheme 3) is much better in terms of frequency dynamic response, and the ESSs and controllable load could indeed improve the dynamic response of frequency regulation.

It is worthy to mention that the proposed distributed hierarchical framework is also very robust to the communication errors and time delay from the tertiary layer and the secondary layer. In the very serious condition that the generation data of both the tertiary and secondary layer or either of them is completely delayed or lost for one DER, the other DERs would pick up this generation shortage, which is very similar to the situation that one DER randomly disconnect from the network. Please refer to the simulation results in Fig.7 for the time period 1300s to 2100s as discussed earlier. Moreover, even for the worst scenario that the generation data in both the tertiary and secondary layer is lost for all DERs, the proposed three hierarchical framework would degrade into a primary frequency regulation layer only, which could also work but with the cost of non-zero frequency deviations.

B. *Case 2: investigate the performance of proposed scheme in 33-bus network with practical load conditions*

In case 2, the following practical load conditions are

settled to validate the performance of proposed scheme: 1) as shown in Fig. 8, the predicted load demand and wind power generation are updated every 300s, and the real time wind power deviations for 3 wind farms (WFs) are generated based on the composite model consisting of the base, the ramp, the gust and the turbulence components [34, 35]; 2) in order to test the plug-in and play capability of proposed scheme, DER11 is plugged out at 6000s and plugged in at 12000s.

Fig. 9 displayed how the 15 DERs were coordinated by the proposed hierarchical scheme to match the real-time load demands and fluctuating wind power generation. As shown in Fig.9a), the tertiary generation regulation layer economically dispatched the predicted load demand by ADMM with a time interval of 300s, while the secondary generation regulation layer further economically conducted generation corrections to timely counterbalance load deviations on top of the tertiary layer in Fig.9b), and finally the 15 DERs actual outputs are obtained in Fig.9c). It is noteworthy that: 1) as DER11 was disconnected during 6000s-12000s, the outputs of DER11 quickly decreased to zero in Fig.9a) to Fig.9c), while for other 14 DERs, their dispatched generations in the tertiary layer, the generation corrections in the secondary layer and their actual outputs obviously increased to a high level for making up the DER11 generation loss; 2) during 6000s-12000s for DER11 disconnection, as DER1 is the most economical generator with the cheapest cost coefficients, its generation output increases extensively even that sometimes DER1 approaches the power upper limit at 750kW. Fig.9d) demonstrates the ESs power outputs and the controllable load level, which indicate that their outputs are always quickly adjusted to counterbalance the frequency deviations.
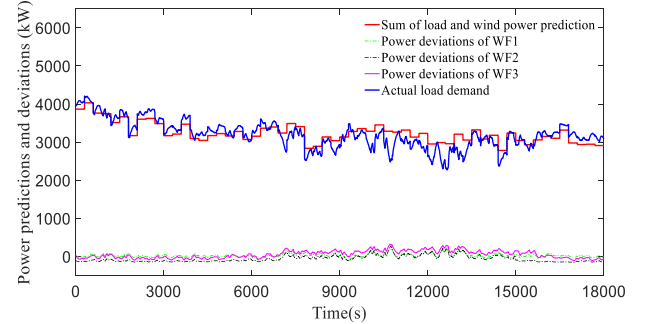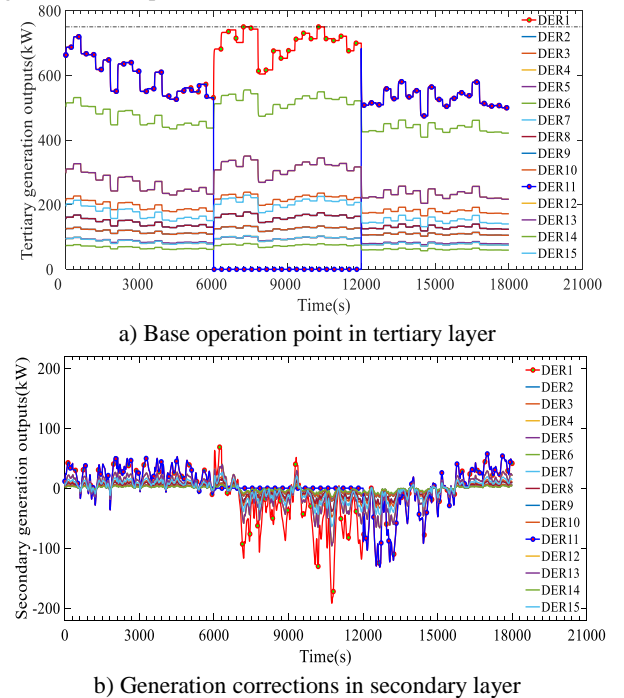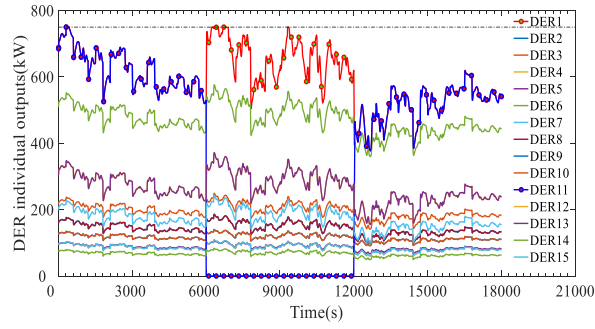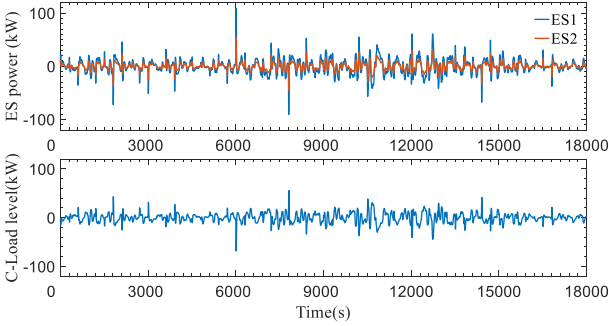

Fig.8 Load/wind prediction and actual deviations for 33-bus ADPN

a) Base operation point in tertiary layer

b) Generation corrections in secondary layer

c) DER actual outputs

d) Energy storage outputs and Controllable load demands
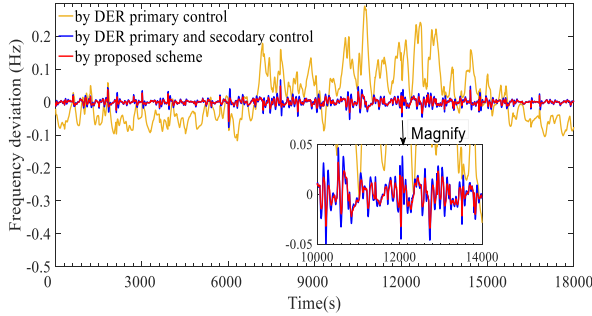Fig.9 DER outputs in 33-bus ADPN with practical load conditions

Fig.10 Frequency regulation in 33-bus ADPN with practical conditions

Fig.10 further compared the frequency regulation performance for three different implementations: 1) the ED algorithm with DER primary frequency droop control only; 2) the proposed three-layer hierarchical control scheme excluding the primary frequency droop control of ESs and controllable load; 3) the proposed completed three-layer hierarchical control scheme. As illustrated by the red line in Fig.10, the proposed distributed scheme could ensure the frequency deviations always in the vicinity of zero with occasionally slight fluctuations not exceeding 0.1Hz. However, the scheme 1) would usually result in non-zero frequency deviations with the maximum as large as 0.3Hz, while scheme 2) also has satisfied frequency regulation performance but worse than the performance of scheme 3). These comparisons demonstrated that for a ADPN with fluctuating wind power generation, as DER generation corrections (on top of the base point in tertiary layer) are conducted in the secondary layer to compensate the fluctuating wind power generation, scheme 2) and 3) can effectively improve the frequency regulation performance, while the later is the most outstanding one because there is plenty of ESs and controllable load with good fast response capability.

V. CASE STUDY FOR 132-BUS WITH LARGE-SCALE DERS

To further investigate the effectiveness of proposed distributed hierarchical scheme to optimally coordinate large-scale DERs, a 132-bus ADPN is deployed with 60 DERs and 12 WFs as shown in Fig.11, which is formed by replicating the aforementioned 33-bus ADPN four times with extra feeders between bus 33 and bus 1. The fuel cost coefficients (a_i, b_i, and c_i) of DERs in area A are the same as

those in case 1,while coefficients for other 45 DERs are partially modified as follows: $1.2a_i$ for DERs in area B, $0.8b_i$ for DERs in area C and $1.5a_i$ for DERs in area D. The predicted load and wind power generation are similarly generated as that for 33-bus ADPN with proportional modifications, which is indicated by the black line in Fig. 12a). The wind power deviations and the ultimately resultant load demand are provided as the pink and green line in Fig.12a). To observe the plug-in/out behaviors of DERs, DER1 in subsystem A is assumed to be plugged out at 9000s and plugged in at 15000s.
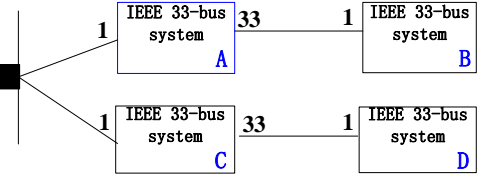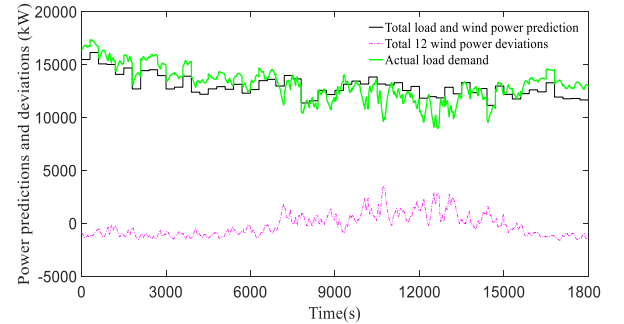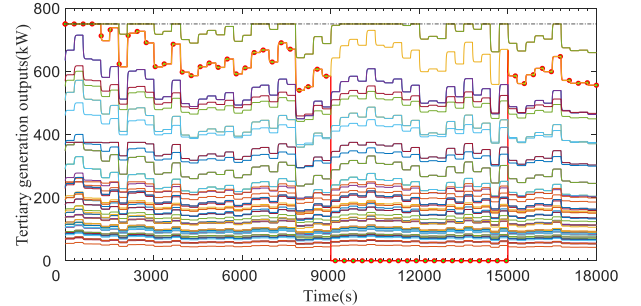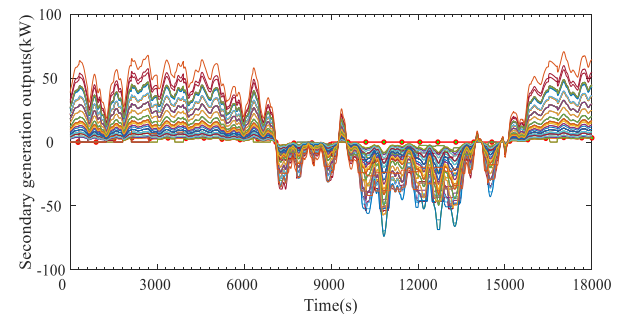

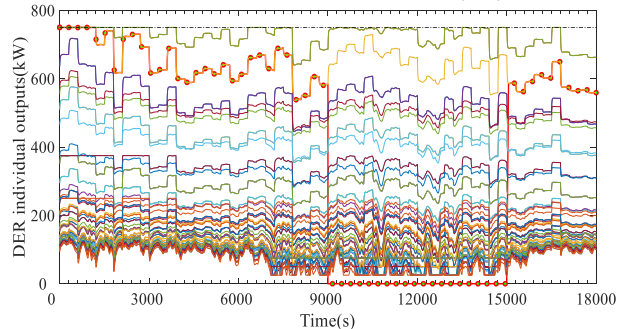Fig.11 Structure of 132-bus ADPN with 60 DERs

a) Predicted load with total wind generation deviations

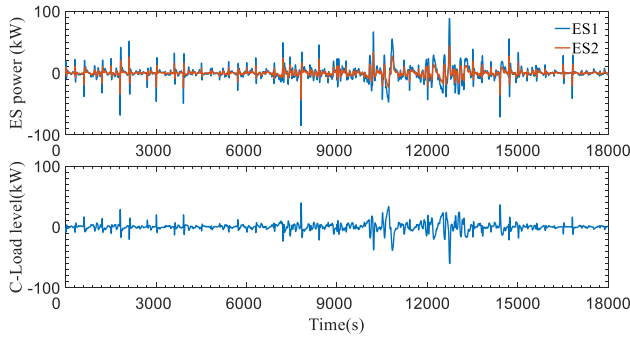b) Base operation point in tertiary layer

c) Generation corrections in secondary layer

d) DER actual outputs

e) ES power outputs and controllable load demand

Fig.12 DER outputs in 132-bus ADPN with practical load conditions

Fig. 12b) to Fig. 12d) demonstrated the optimized base operation point in tertiary regulation layer, the generation corrections in secondary regulation layer and the actual generation outputs of 60 DERs solved by the proposed hierarchical scheme. As illustrated by these figures, the tertiary layer could effectively address the optimal base point according to the predicted load demand and wind power generation, while the secondary generation regulation layer could further economically conduct generation corrections on top of tertiary generation regulation, and finally the outputs of 60 DERs are coordinated to match the real time load demands of 132-bus ADPN as shown in Fig. 12d). It is also noted that when DER1 is disconnected during 9000s-15000s, the optimal generation base point in tertiary layer, the generation corrections of secondary layer and the actual generation outputs for DER1 are all decreased to zero. And the proposed scheme is still effective to guide other 59 DERs to seek the optimal outputs for minimizing the fuel cost and regulating system frequency well. As DER41 is much cheaper than other DERs, its generation output is very large and frequently restricted by the upper generation limit, while DER7, 8, 9, 10, 34, 35, 37 and 39 etc. occasionally reach their lower generation limits during 7000s-14000s as shown in Fig. 12d) because of their expensive marginal fuel costs. Fig.12e) also demonstrates the ESs power outputs and the controllable load level accordingly during the procedure of counterbalancing the frequency deviations.
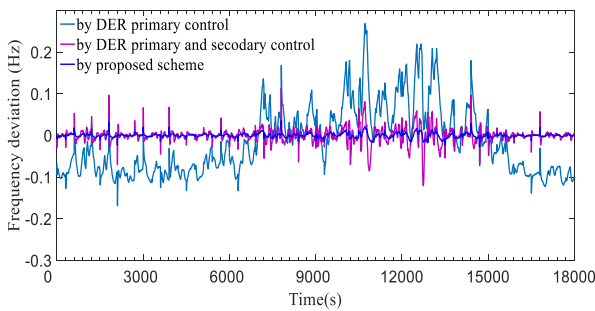

Fig.13 Frequency regulation performance for 132-bus ADPN

Fig. 13 plotted the frequency deviations of 132-bus ADPN for three different schemes: 1) the ED algorithm with DER primary frequency droop control; 2) the proposed three-layer hierarchical control scheme without the primary frequency droop control of ESs and controllable load; 3) the proposed completed three-layer hierarchical control scheme. It is evident that the proposed scheme 3) can effectively regulate the system frequency and the maximal frequency deviation is near zero as the blue line shown in Fig. 13. However, the scheme 1) or 2) could only regulate the system at large non-zero frequency deviations. These simulation results demonstrated that the proposed scheme is the best one capable of effectively regulating the system frequency.

VI. CONCLUSION

In this paper, a fully distributed three-layer control framework is proposed for the coordinated operation of multiple DERs in ADPN. Based on the discrete finite-time consensus algorithm, a fully distributed dispatch scheme and a fair generation correction strategy are designed in the tertiary and secondary generation regulation layer respectively. While in the primary generation regulation layer, a frequency droop controller is presented to ensure DERs outputs perfectly tracking the power reference of the tertiary and secondary layers, and DERs with energy storage and controllable load could well maintain satisfactory system dynamic frequency in real time. Tests on the modified IEEE 33-bus and 132-bus ADPN with large-scale DERs have demonstrated the effectiveness of the proposed control scheme in optimally coordinating DERs outputs, ensuring satisfactory system frequency and robustly accommodating uncertainties of DERs. Since the proposed fully distributed hierarchical scheme to exclusively regulate system frequency may result in operation constraint violations, such as violating the voltage or line capacity limits, further ongoing research would elaborately design an all-round distributed hierarchical scheme (e.g., based on fully distributed optimal power flow model) to simultaneously regulate system frequency and ensure static security of distribution networks.

VII. ACKNOWLEDGMENT

VIII. REFERENCE

[1] X. Shen, M. Shahidehpour, S. Zhu, Y. Han, and J. Zheng, "Multi-Stage Planning of Active Distribution Networks Considering the Co-Optimization of Operation Strategies," *IEEE Trans. Smart Grid,* vol. 9, no. 2, pp. 1425-1433, Mar. 2018.

[2] A. Madureira, C. Gouveia, C. Moreira, L. Seca, and J. P. Lopes, "Coordinated management of distributed energy resources in electrical distribution systems," in *Proc. 2013 IEEE PES Conference on Innovative Smart Grid Technologies (ISGT Latin America)*, 15-17 April 2013, pp. 1-8.

[3] W. Zheng, W. Wu, B. Zhang, H. Sun, and Y. Liu, "A Fully Distributed Reactive Power Optimization and Control Method for Active Distribution Networks," *IEEE Trans. Smart Grid,* vol. 7, no. 2, pp. 1021-1033, Mar. 2016.

[4] Q. Shafiee, V. Nasirian, J. C. Vasquez, J. M. Guerrero, and A. Davoudi, "A Multi-Functional Fully Distributed Control Framework for AC Microgrids," *IEEE Trans. Smart Grid,* vol. PP, no. 99, p. 1-1, 2017.

[5] W. T. Elsayed and E. F. El-Saadany, "A Fully Decentralized Approach for Solving the Economic Dispatch Problem," *IEEE Trans. Power Systems,* vol. 30, no. 4, pp. 2179-2189, July 2015.

[6] S. Yang, S. Tan, and J. Xu, "Consensus Based Approach for Economic Dispatch Problem in a Smart Grid," *IEEE Trans. Power Systems,* vol. 28, no. 4, pp. 4416-4426, Nov. 2013.

[7] Z. Zhang and M. Chow, "Convergence Analysis of the Incremental Cost Consensus Algorithm Under Different Communication Network Topologies in a Smart Grid," *IEEE Trans. Power Systems,* vol. 27, no. 4, pp. 1761-1768, Nov. 2012.

[8] H. Pourbabak, J. Luo, T. Chen, and W. Su, "A Novel Consensus-based Distributed Algorithm for Economic Dispatch Based on Local Estimation of Power Mismatch," *IEEE Trans. Smart Grid,* vol. PP, no.

99, p. 1-1, 2017.

[9] G. Hug, S. Kar, and C. Wu, "Consensus Innovations Approach for Distributed Multiagent Coordination in a Microgrid," *IEEE Trans. Smart Grid,* vol. 6, no. 4, pp. 1893-1903, Jul. 2015.

[10] S. Kar and G. Hug, "Distributed robust economic dispatch in power systems: A consensus+innovations approach," in *Proc. 2012 IEEE Power and Energy Society General Meeting*, 22-26 July 2012, pp. 1-8.

[11] Y. Wang, L. Wu, and S. Wang, "A Fully-Decentralized Consensus-Based ADMM Approach for DC-OPF With Demand Response," *IEEE Trans. Smart Grid,* vol. 8, no. 6, pp. 2637-2647, Nov. 2017.

[12] L. Meng, T. Dragicevic, J. Vasquez, J. Guerrero, and E. R. Sanseverino, "Hierarchical control with virtual resistance optimization for efficiency enhancement and State-of-Charge balancing in DC microgrids," in *Proc. 2015 IEEE First International Conference on DC Microgrids (ICDCM)*, 7-10 June 2015, pp. 1-6.

[13] A. Mehrizi-Sani and R. Iravani, "Potential-Function Based Control of a Microgrid in Islanded and Grid-Connected Modes," *IEEE Trans. Power Systems,* vol. 25, no. 4, pp. 1883-1891, Nov. 2010.

[14] J. Tan and L. Wang, "A Game-Theoretic Framework for Vehicle-to-Grid Frequency Regulation Considering Smart Charging Mechanism," *IEEE Trans. Smart Grid,* vol. PP, no. 99, pp. 1-12, 2016.

[15] J. Tan and L. Wang, "Coordinated optimization of PHEVs for frequency regulation capacity bids using hierarchical game," in *Proc. 2015 IEEE PES General Meeting*, Jul. 2015, pp. 1-5.

[16] J. W. Simpson-Porco, Q. Shafiee, F. Dörfler, J. C. Vasquez, J. M. Guerrero, and F. Bullo, "Secondary Frequency and Voltage Control of Islanded Microgrids via Distributed Averaging," *IEEE Trans. Industrial Electronics,* vol. 62, no. 11, pp. 7025-7038, Nov. 2015.

[17] X. Lu, X. Yu, J. Lai, J. M. Guerrero, and H. Zhou, "Distributed Secondary Voltage and Frequency Control for Islanded Microgrids With Uncertain Communication Links," *IEEE Trans. Industrial Informatics,* vol. 13, no. 2, pp. 448-460, Apr. 2017.

[18] M. A. Mahmud, M. J. Hossain, H. R. Pota, and N. K. Roy, "Nonlinear distributed controller design for maintaining power balance in Islanded microgrids," in *Proc. 2014 IEEE PES General Meeting | Conference & Exposition*, 27-31 July 2014, pp. 1-5.

[19] Q. Shafiee, J. M. Guerrero, and J. C. Vasquez, "Distributed Secondary Control for Islanded Microgrids-A Novel Approach," *IEEE Trans. Power Electronics,* vol. 29, no. 2, pp. 1018-1031, Feb. 2014.

[20] A. J. Wood and B. F. Wollenberg, *Power generation, operation, and control*: John Wiley & Sons, 2012.

[21] X. Luo, S. W. Xia, K. W. Chan, and X. Lu, "A Hierarchical Scheme for Utilizing Plug-In Electric Vehicle Power to Hedge Against Wind-Induced Unit Ramp Cycling Operations," *IEEE Transactions on Power Systems,* vol. 33, no. 1, pp. 55-69, Jan. 2018.

[22] E. Ela and M. O'Malley, "Studying the Variability and Uncertainty Impacts of Variable Generation at Multiple Timescales," *IEEE Transactions on Power Systems,* vol. 27, no. 3, pp. 1324-1333, Aug. 2012.

[23] A. Y. Kibangou, "Graph Laplacian based matrix design for finite-time distributed average consensus," in *Proc. 2012 American Control Conference (ACC)*, 27-29 June 2012, pp. 1901-1906.

[24] T. M. D. Tran and A. Y. Kibangou, "Distributed Estimation of Graph Laplacian Eigenvalues by the Alternating Direction of Multipliers Method," *IFAC Proceedings,* vol. 47, no. 3, pp. 5526-5531, 2014.

[25] A. Y. Kibangou and C. Commault, "Decentralized Laplacian Eigenvalues Estimation and Collaborative Network Topology Identification," *IFAC Proceedings,* vol. 45, no. 26, pp. 7-12, 2012.

[26] E. Ghadimi, A. Teixeira, I. Shames, and M. Johansson, "Optimal parameter selection for the alternating direction method of multipliers (ADMM): quadratic problems," *IEEE Trans. Automatic Control,* vol. 60, no. 3, pp. 644-658, Mar. 2015.

[27] T. H. Chang, M. Hong, and X. Wang, "Multi-Agent Distributed Optimization via Inexact Consensus ADMM," *IEEE Trans. Signal Processing,* vol. 63, no. 2, pp. 482-497, Jan. 2015.

[28] S. Boyd, N. Parikh, E. Chu, B. Peleato, and J. Eckstein, "Distributed optimization and statistical learning via the alternating direction method of multipliers," *Foundations and Trends in Communications and Information Theory,* vol. 1, no. 3, pp. 1-122, 2011.

[29] A. Khalil and Z. Rajab, "Load frequency control system with smart meter and controllable loads," in *Proc. The 8th International Renewable Energy Congress (IREC 2017)*, Amman, Jordan, 21-23 March 2017, pp. 1-5.

[30] C. Jiang, B. Li, and J. Shen, "Controllable Load Management Approaches in Smart Grids," *Energies,* vol. 2015, no. 8, pp. 11187-11202, 2015.

[31] T. Kim and W. Qiao, "A Hybrid Battery Model Capable of Capturing Dynamic Circuit Characteristics and Nonlinear Capacity Effects," *IEEE Transactions on Energy Conversion,* vol. 26, no. 4, pp. 1172-1180, Dec. 2011.

[32] V. B., C. S., K. N., and P. K. D. R., "Optimal reconfiguration of radial distribuion system using artificial intelligence methods," in *Proc. 2009 IEEE Toronto International Conference Science and Technology for Humanity*, 26-27 Sept. 2009, pp. 660-665.

[33] S. J. Ahn, S. R. Nam, J. H. Choi, and S. I. Moon, "Power Scheduling of Distributed Generators for Economic and Stable Operation of a Microgrid," *IEEE Trans. Smart Grid,* vol. 4, no. 1, pp. 398-405, Mar. 2013.

[34] X. Luo, S. Xia, and K. W. Chan, "A decentralized charging control strategy for plug-in electric vehicles to mitigate wind farm intermittency and enhance frequency regulation," *Journal of Power Sources,* vol. 248, pp. 604-614, Feb. 2014.

[35] F. Milano, "An Open Source Power System Analysis Toolbox," *IEEE Trans. Power Systems,* vol. 20, no. 3, pp. 1199-1206, Aug. 2005.
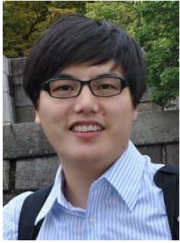
IX.   BIOGRAPHY

Shiwei Xia (M'12) received the B.Eng. and M.Eng. degrees in electrical engineering from Harbin Institute of Technology, Harbin, China, in 2007 and 2009 respectively, and the Ph.D. degree in power systems from The Hong Kong Polytechnic University, Hung Hom, Hong Kong, in 2015. Then, he worked as a Research Associate and subsequently as a Postdoctoral Fellow with the Department of Electrical Engineering, The Hong Kong Polytechnic University, in 2016-2018. Currently, he is with the State Key Laboratory of Alternate Electrical Power System with Renewable Energy Sources, School of Electrical and Electronic Engineering, North China Electric Power University, Beijing, and also with The Hong Kong Polytechnic University, Hong Kong. His research interests include security and risk analysis for power systems with renewable energies, distributed optimization and control of multiple sustainable energy sources in active distribution network. smart grid.

S. Q. Bu (S'11-M'12-SM'17) received the Ph.D. degree from the electric power and energy research cluster, The Queen's University of Belfast, Belfast, U.K., in 2012, where he continued his postdoctoral research work before entering industry. Subsequently, he joined National Grid UK as a Power System Engineer and then became an experienced UK National Transmission System Planner and Operator. He is an Assistant Professor with The Hong Kong Polytechnic University, Kowloon, Hong Kong, and also a Chartered Engineer with UK Engineering Council, London, U.K.. His research interests are power system stability analysis and operation control, including wind power generation, PEV, HVDC, FACTS, ESS and VSG.

He has received various prizes due to excellent performances and outstanding contributions in operational and commissioning projects during the employment with National Grid UK. He is also the recipient of Outstanding Reviewer Awards from IEEE Transactions on Sustainable Energy, IEEE Transactions on Power Systems, Renewable Energy and International Journal of Electrical Power and Energy Systems.

Can Wan (M'15) received his B.Eng. and Ph.D. degrees from Zhejiang University, China, in 2008, and The Hong Kong Polytechnic University in 2015, respectively.

He is a Research Professor with College of Electrical Engineering, Zhejiang University, Hangzhou, China, under the university Hundred Talents Program. He was a Postdoc Fellow at Department of Electrical Engineering, Tsinghua University, Beijing, China, and held research positions at Technical University of Denmark, The Hong Kong Polytechnic University, and City University of Hong Kong. He was a visiting scholar at the Center for Electric Power and Energy, Technical University of Denmark, and Argonne National Laboratory, IL, USA. His research interests include forecasting, renewable energy, active distribution network, integrated energy systems, and machine learning.

Xi Lu received the B.Eng. degree in Electrical Engineering from North China Electric Power University in Beijing, China in 2015. He is currently pursuing the PhD degree in Electrical Engineering at the Hong Kong Polytechnic University, Hong Kong. His research interests include application of robust optimization and distributionally robust optimization in power system operation.

Ka Wing Chan (M'98) received the B.Sc. (Hons) and Ph.D. degrees in electronic and electrical engineering from the University of Bath, U.K., in 1988 and 1992, respectively. He currently is an Associate Professor and Associate Head in the Department of Electrical Engineering of the Hong Kong Polytechnic University. His general research interests include power system stability, analysis and control, power grid integration, security, resilience and optimization, demand response management.

Bin Zhou (S'11-M'13-SM'17) received the B.Sc. degree in electrical engineering from Zhengzhou University, Zhengzhou, China, in 2006, the M.S. degree in electrical engineering from South China University of Technology, Guangzhou, China, in 2009, and the Ph.D. degree from The Hong Kong Polytechnic University, Hong Kong, in 2013. Afterwards, he worked as a Research Associate and subsequently a Postdoctoral Fellow in the Department of Electrical Engineering of The Hong Kong Polytechnic University. Now, he is an Associate Professor in the College of Electrical and Information Engineering, Hunan University, Changsha, China. His main fields of research include smart grid operation and planning, renewable energy generation, and energy efficiency.